

Electronic Supplementary Information (ESI)

## Ester-functionalized thermally activated delayed fluorescence materials

Hiroshi Tasaki,<sup>ab</sup> So Shikita,<sup>ab</sup> In Seob Park<sup>a</sup> and Takuma Yasuda<sup>\*ab</sup>

<sup>a</sup> INAMORI Frontier Research Center (IFRC), Kyushu University,  
744 Motoooka, Nishi-ku, Fukuoka 819-0395, Japan

<sup>b</sup> Department of Applied Chemistry, Graduate School of Engineering,  
Kyushu University, 744 Motoooka, Nishi-ku, Fukuoka 819-0395, Japan

E-mail: yasuda@ifrc.kyushu-u.ac.jp

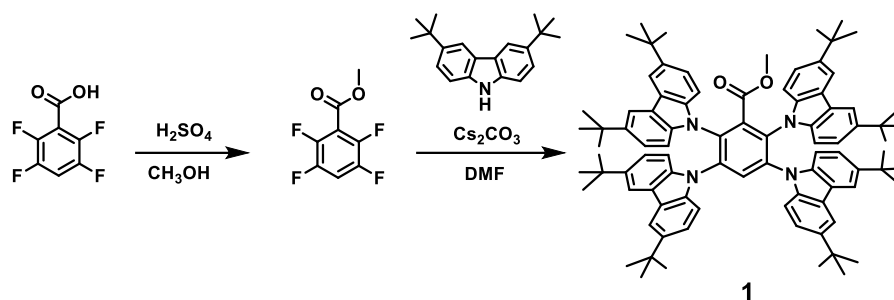
### Contents:

<b>Materials, Synthesis, and Characterization</b> .....	S2–S6
<b>Computational Simulations</b> .....	S7
<b>Photophysical Measurements</b> .....	S7
<b>OLED Fabrication and Evaluation</b> .....	S7
<b>Figures S1–S8.</b> <sup>1</sup> H and <sup>13</sup> C{ <sup>1</sup> H} NMR and MALDI-TOF-MS spectra .....	S8–S15
<b>Figures S9–S10.</b> Computational results .....	S16
<b>Figure S11.</b> Transient PL characteristics in solution .....	S17
<b>Figure S12.</b> UV–vis absorption and PL spectra in solution .....	S17
<b>Figure S13.</b> Solvatochromic PL properties .....	S18
<b>Figure S14.</b> AIE characteristics in THF/water mixtures .....	S18
<b>Figure S15.</b> Temperature-dependence of transient PL characteristics .....	S19
<b>Figure S16.</b> Photophysical characteristics of <b>5BCzBN</b> in the neat films .....	S19
<b>Figure S17.</b> Energy-level diagram of OLEDs (device A–E) .....	S20
<b>Figure S18.</b> EL characteristics of device E .....	S20
<b>References</b> .....	S21

## Materials, Synthesis, and Characterization

All reagents and anhydrous solvents were purchased from Sigma-Aldrich, Tokyo Chemical Industry (TCI), or Fujifilm Wako Pure Chemical Corp., and were used without further purification unless otherwise noted. 1,3-Bis[3,5-di(pyridin-3-yl)phenyl]benzene (B3PyPB),<sup>[S1]</sup> 9-phenyl-3,9'-bicarbazole (CCP),<sup>[S2]</sup> and 2,3,4,5,6-pentakis(3,6-di-*tert*-butylcarbazol-9-yl)benzotrile (**5BCzBN**)<sup>[S3]</sup> were prepared according to the literature procedures, and purified by temperature-gradient vacuum sublimation before use. 2,3,6,7,10,11-Hexacyano-1,4,5,8,9,12-hexaazatriphenylene (HAT-CN), 1,1-bis[4-[*N,N*-di(*p*-tolyl)amino]phenyl]cyclohexane (TAPC), 2,8-bis(diphenylphosphinyl)dibenzo[*b,d*]furan (PPF), and 8-quinolinolato lithium (Liq) were purchased from LG Chem Ltd., Luminescence Technology Corp., TCI, and e-Ray Optoelectronics Technology Co., Ltd., respectively, and used without further purification.

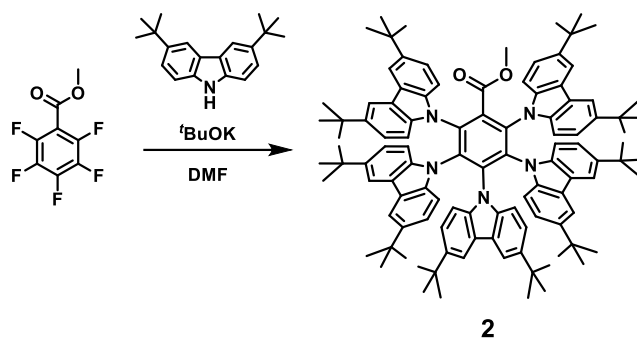
NMR spectra were recorded on an Avance III 400 spectrometer (Bruker). Chemical shifts were referenced to tetramethylsilane ( $\delta = 0.00$ ) for <sup>1</sup>H NMR and CDCl<sub>3</sub> ( $\delta = 77.0$ ) for <sup>13</sup>C{<sup>1</sup>H} NMR as internal standards. Matrix-assisted laser desorption ionization time-of-flight (MALDI-TOF) mass spectra were collected on an Autoflex III spectrometer (Bruker Daltonics) using dithranol as a matrix. Atmospheric pressure chemical ionization (APCI) mass spectra were measured using an Advion expression CMS-L spectrometer (Biotage). Elemental analyses were carried out using an MT-5 analyzer (Yanaco).



**Scheme S1.** Synthesis of **1**.

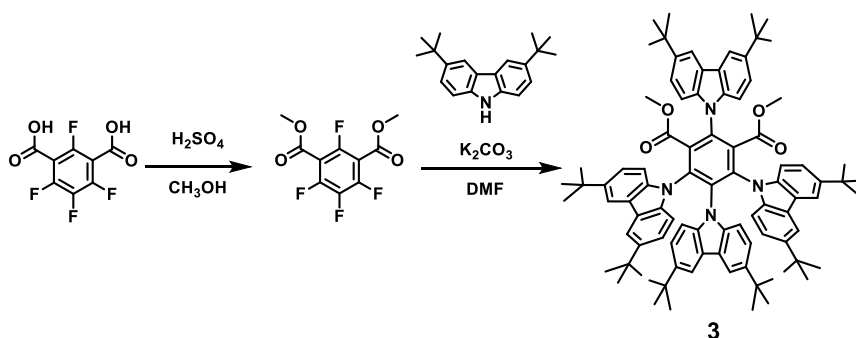
**Synthesis of methyl 2,3,5,6-tetrafluorobenzoate:** A mixture of methyl-2,3,5,6-tetrafluorobenzoic acid (7.76 g, 40.0 mmol) and H<sub>2</sub>SO<sub>4</sub> (12 mL) in dry CH<sub>3</sub>OH (50 mL) was refluxed for 46 h. After cooling to room temperature, the reaction mixture was concentrated under reduced pressure. The resulting mixture was neutralized with an aqueous solution of NaHCO<sub>3</sub> and then extracted with CH<sub>2</sub>Cl<sub>2</sub>. The combined organic layer was dried with anhydrous Na<sub>2</sub>SO<sub>4</sub>, filtrated, and concentrated under reduced pressure. The crude product was purified by column chromatography on silica gel (eluent: CH<sub>2</sub>Cl<sub>2</sub>) to afford methyl 2,3,5,6-tetrafluorobenzoate as a yellow liquid (yield = 6.32 g, 76%). <sup>1</sup>H NMR (400 MHz, CDCl<sub>3</sub>): δ 7.25-7.16 (m, 1H), 3.99 (s, 3H). MS (APCI): *m/z* calcd 208.11 [*M*]<sup>+</sup>; found 209.0.

**Synthesis of 4BCzMB (1):** A mixture of 3,6-di-*tert*-butylcarbazole (4.59 g, 16.4 mmol) and Cs<sub>2</sub>CO<sub>3</sub> (5.35 g, 16.4 mmol) in dry DMF (64 mL) was stirred for 3 h at room temperature. After the addition of a solution of methyl 2,3,5,6-tetrafluorobenzoate (0.835 g, 4.01 mmol) in dry DMF (16 mL), the mixture was stirred for 24 h at 80 °C. After cooling to room temperature, the reaction mixture was added into water and extracted with CHCl<sub>3</sub>. The combined organic layer was washed with water and dried over anhydrous Na<sub>2</sub>SO<sub>4</sub>. After filtration and evaporation, the crude product was purified by column chromatography on silica gel (eluent: CH<sub>2</sub>Cl<sub>2</sub>), followed by recycling preparative GPC (eluent: CHCl<sub>3</sub>) to afford **1** as a yellow solid (yield = 1.35 g, 27%). <sup>1</sup>H NMR (400 MHz, CDCl<sub>3</sub>): δ 8.23 (s, 1H), 7.65 (d, *J* = 1.6 Hz, 4H), 7.61 (d, *J* = 1.2 Hz, 4H), 7.09-6.99 (m, 16H), 2.77 (s, 3H), 1.35 (s, 36H), 1.34 (s, 36H). <sup>13</sup>C{<sup>1</sup>H} NMR (100 MHz, CDCl<sub>3</sub>): δ 164.66, 143.06, 142.84, 138.58, 138.33, 138.23, 136.93, 133.48, 133.20, 124.00, 123.81, 122.80, 122.75, 115.51, 115.33, 109.93, 109.26, 52.38, 34.50, 31.91. MS (MALDI-TOF): *m/z* calcd 1244.78 [*M*]<sup>+</sup>; found 1244.40. Anal. calcd (%) for C<sub>88</sub>H<sub>100</sub>N<sub>4</sub>O<sub>2</sub>: C 84.84, H 8.09, N 4.50; found: C 84.25, H 8.10, N 4.40.



**Scheme S2.** Synthesis of **2**.

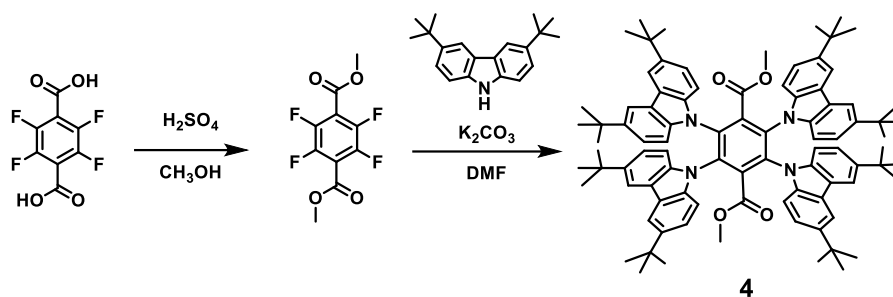
**Synthesis of 5BCzMB (2):** A mixture of 3,6-di-*tert*-butylcarbazole (2.85 g, 10.2 mmol) and *t*BuOK (1.14 g, 10.2 mmol) in dry DMF (40 mL) was stirred for 3 h at room temperature. After the addition of a solution of methyl 2,3,4,5,6-pentafluorobenzoate (0.45 g, 1.99 mmol) in dry DMF (10 mL), the mixture was stirred for 18 h at 80 °C. After cooling to room temperature, the reaction mixture was added into water and extracted with ethyl acetate. The combined organic layer was dried over anhydrous Na<sub>2</sub>SO<sub>4</sub>. After filtration and evaporation, the crude product was purified by column chromatography on silica gel (eluent: hexane/CHCl<sub>3</sub> = 3:1, v/v) to afford **2** as a yellow solid (yield = 1.48 g, 49%). <sup>1</sup>H NMR (400 MHz, CDCl<sub>3</sub>): δ 7.63 (d, *J* = 1.5 Hz, 4H), 7.23-7.22 (m, 6H), 7.04-6.97 (m, 10H), 6.88 (d, *J* = 8.5 Hz, 4H), 6.62-6.58 (m, 6H), 2.53 (s, 3H), 1.31 (s, 36H), 1.22 (s, 36H), 1.18 (s, 18H). <sup>13</sup>C{<sup>1</sup>H} NMR (100 MHz, CDCl<sub>3</sub>): δ 164.22, 142.65, 142.53, 142.35, 139.12, 138.52, 137.43, 137.39, 136.63, 135.77, 135.68, 124.17, 124.04, 123.88, 122.63, 121.98, 121.80, 115.39, 114.88, 114.74, 110.32, 110.14, 109.71, 52.02, 34.45, 34.22, 31.88, 31.77, 31.72. MS (MALDI-TOF): *m/z* calcd 1521.97 [*M*]<sup>+</sup>; found 1521.52. Anal. calcd (%) for C<sub>108</sub>H<sub>123</sub>N<sub>5</sub>O<sub>2</sub>: C 85.16, H 8.14, N 4.60; found: C 84.96, H 8.09, N 4.66.



**Scheme S3.** Synthesis of **3**.

**Synthesis of dimethyl 2,4,5,6-tetrafluoroisophthalate:** A mixture of tetrafluoroisophthalic acid (4.76 g, 20.0 mmol) and H<sub>2</sub>SO<sub>4</sub> (6 mL) in dry CH<sub>3</sub>OH (25 mL) was refluxed for 47 h. After cooling to room temperature, the reaction mixture was concentrated under reduced pressure. The resulting mixture was neutralized with an aqueous solution of NaHCO<sub>3</sub> and then extracted with CH<sub>2</sub>Cl<sub>2</sub>. The combined organic layer was dried with anhydrous Na<sub>2</sub>SO<sub>4</sub>, filtrated, and concentrated under reduced pressure. The crude product was purified by column chromatography on silica gel (eluent: CH<sub>2</sub>Cl<sub>2</sub>) to afford dimethyl 2,4,5,6-tetrafluoroisophthalate as a light brown liquid (yield = 3.87 g, 73%). <sup>1</sup>H NMR (400 MHz, CDCl<sub>3</sub>): δ 3.97 (s, 6H). MS (APCI): *m/z* calcd 266.15 [*M*]<sup>+</sup>; found 266.8.

**Synthesis of 4BCzDMI (3):** A mixture of 3,6-di-*tert*-butylcarbazole (5.73 g, 20.5 mmol) and K<sub>2</sub>CO<sub>3</sub> (2.83 g, 20.5 mmol) in dry DMF (65 mL) was stirred for 3 h at room temperature. After the addition of a solution of dimethyl 2,4,5,6-tetrafluoroisophthalate (1.33 g, 5.00 mmol) in dry DMF (15 mL), the mixture was stirred for 67 h at 80 °C. After cooling to room temperature, the reaction mixture was added into water and extracted with CHCl<sub>3</sub>. The combined organic layer was dried over anhydrous Na<sub>2</sub>SO<sub>4</sub>. After filtration and evaporation, the crude product was purified by column chromatography on silica gel (eluent: hexane/CHCl<sub>3</sub> = 3:1, v/v), followed by recycling preparative GPC (eluent: CHCl<sub>3</sub>) to afford **3** as a yellow solid (yield = 1.32 g, 20%). <sup>1</sup>H NMR (400 MHz, CDCl<sub>3</sub>): δ 8.06 (d, *J* = 1.8 Hz, 6H), 8.04 (d, *J* = 1.8 Hz, 2H), 7.51 (d, *J* = 1.8 Hz, 2H), 7.49 (d, *J* = 1.8 Hz, 4H), 7.47 (d, *J* = 2.0 Hz, 2H), 7.23-7.20 (m, 8H), 2.66 (s, 6H), 1.43 (s, 72H). <sup>13</sup>C{<sup>1</sup>H} NMR (100 MHz, CDCl<sub>3</sub>): δ 162.93, 143.84, 143.22, 140.62, 139.24, 136.61, 131.79, 131.74, 128.07, 127.93, 124.05, 123.88, 123.57, 116.40, 116.00, 109.63, 109.22, 52.40, 34.76, 34.72, 31.98, 31.95. MS (MALDI-TOF): *m/z* calcd 1302.79 [*M*]<sup>+</sup>; found 1302.61.



**Scheme S4.** Synthesis of **4**.

**Synthesis of dimethyl 2,3,5,6-tetrafluoroterephthalate:** A mixture of tetrafluoroterephthalic acid (11.9 g, 50.0 mmol) and H<sub>2</sub>SO<sub>4</sub> (15 mL) in dry CH<sub>3</sub>OH (63 mL) was refluxed for 47 h. After cooling to room temperature, the reaction mixture was concentrated under reduced pressure. The resulting mixture was neutralized with an aqueous solution of NaHCO<sub>3</sub> and then extracted with CH<sub>2</sub>Cl<sub>2</sub>. The combined organic layer was dried with anhydrous Na<sub>2</sub>SO<sub>4</sub>, filtrated, and concentrated under reduced pressure. The crude product was purified by column chromatography on silica gel (eluent: hexane/CHCl<sub>3</sub> = 1:1, v/v) to afford dimethyl 2,3,5,6-tetrafluoroterephthalate as a white solid (yield = 11.0 g, 83%). <sup>1</sup>H NMR (400 MHz, CDCl<sub>3</sub>): δ 4.01 (s, 6H). MS (MALDI-TOF): *m/z* calcd 266.02 [*M*]<sup>+</sup>; found 266.24.

**Synthesis of 4BCzDMT (4):** A mixture of 3,6-di-*tert*-butylcarbazole (1.15 g, 4.12 mmol) and K<sub>2</sub>CO<sub>3</sub> (0.568 g, 4.11 mmol) in dry DMF (13 mL) was stirred for 3 h at room temperature. After the addition of a solution of dimethyl 2,3,5,6-tetrafluoroterephthalate (0.267 g, 1.00 mmol) in dry DMF (4 mL), the mixture was stirred for 19 h at 110 °C. After cooling to room temperature, the reaction mixture was added into water and extracted with CHCl<sub>3</sub>. The combined organic layer was dried over anhydrous Na<sub>2</sub>SO<sub>4</sub>. After filtration and evaporation, the crude product was purified by column chromatography on silica gel (eluent: hexane/CHCl<sub>3</sub> = 3:1, v/v), followed by recycling preparative GPC (eluent: CHCl<sub>3</sub>) to afford **4** as a yellowish white solid (yield = 0.58 g, 44%). <sup>1</sup>H NMR (400 MHz, CDCl<sub>3</sub>): δ 7.57-7.58 (m, 8H), 7.04-6.99 (m, 16H), 2.73 (s, 6H), 1.34 (s, 72H). <sup>13</sup>C{<sup>1</sup>H} NMR (100 MHz, CDCl<sub>3</sub>): δ 163.91, 142.80, 139.81, 138.65, 135.97, 123.84, 122.62, 115.22, 109.87, 52.41, 34.47, 31.90. MS (MALDI-TOF): *m/z* calcd 1302.79 [*M*]<sup>+</sup>; found 1302.44. Anal. calcd (%) for C<sub>90</sub>H<sub>102</sub>N<sub>4</sub>O<sub>4</sub>: C 82.91, H 7.89, N 4.30; found: C 82.80, H 7.85, N 4.37.

## Computational Simulations

All quantum chemical calculations on the basis of time-dependent density functional theory (TD-DFT) were performed using the Gaussian16 program package.<sup>[S4]</sup> The ground-state ( $S_0$ ) geometries for the emitters were initially optimized using the PBE0 functional with the 6-31G(d) basis set in the gas phase. The vertical excitation calculations were carried out using the optimized  $S_0$  geometries, and the geometry optimizations in the excited  $S_1$  and  $T_1$  states were performed using TD-DFT at the same level of theory. For the  $S_0 \rightarrow S_1$  and  $S_0 \rightarrow T_1$  transitions, the natural transition orbitals (NTOs) with their adiabatic excitation energies were simulated using the optimized  $S_1$  and  $T_1$  geometries, respectively.

## Photophysical Measurements

Thin-film samples for photophysical measurements were prepared on quartz substrates through vacuum deposition ( $<7 \times 10^{-5}$  Pa) using an E-200 vacuum evaporation system (ALS Technology). UV-vis absorption and PL spectra were measured using a V-670 spectrometer (Jasco) and an FP-8600 spectrophotometer (Jasco), respectively. The absolute PL quantum yields ( $\Phi_{\text{PL}}$ ) were determined with an ILF-835 integrating sphere system (Jasco). The transient PL decay measurements were performed using a C11367 Quantaaurus-tau fluorescence lifetime spectrometer (Hamamatsu Photonics;  $\lambda_{\text{ex}} = 280$  nm, pulse width  $< 1$  ns, and repetition rate = 50 kHz) under  $\text{N}_2$  for solutions or vacuum ( $<10^{-1}$  Pa) for thin-film samples. The emission lifetimes were determined from the resulting PL decay curves by performing exponential fitting and deconvolution with the instrument response function.

## OLED Fabrication and Evaluation

ITO-coated glass substrates were cleaned with detergent, deionized water, acetone, and isopropanol in this order. The substrates were then subjected to UV-ozone treatment for 15 min before being loaded into an E-200 vacuum evaporation system (ALS Technology). The organic layers and a cathode Al layer were thermally evaporated on the substrates under vacuum ( $<6 \times 10^{-5}$  Pa) with a deposition rate of  $<0.3$  nm  $\text{s}^{-1}$  through a shadow mask, defining a pixel size of  $0.04$  cm<sup>2</sup>. The thickness and deposition rate were monitored *in situ* during deposition by oscillating quartz thickness monitors. The  $J$ - $V$ - $L$  characteristics and angle-resolved EL intensities of the fabricated OLEDs were measured using a 2400 source meter (Keithley) and a CS-2000 spectroradiometer (Konica Minolta). The EL efficiencies of the fabricated devices were corrected by the Lambertian factors estimated from the angle-resolved EL data.

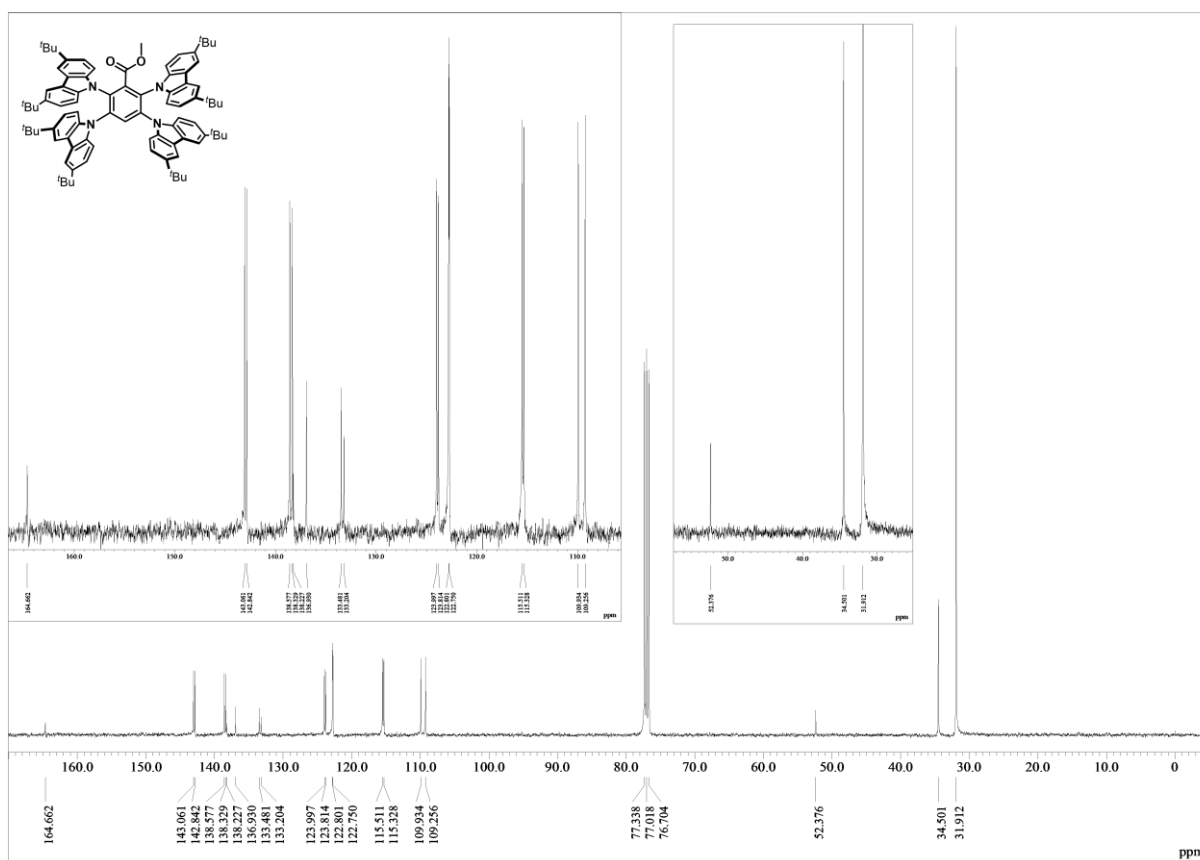
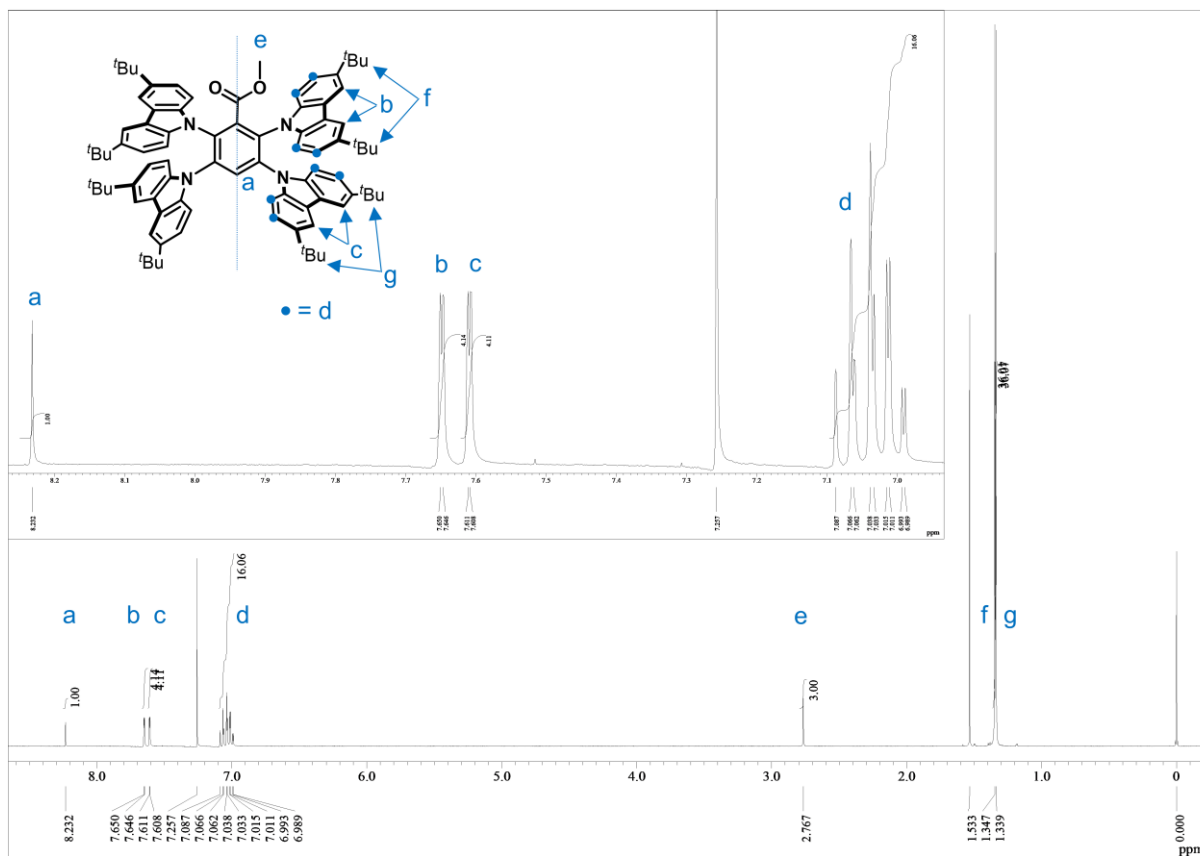


**Figure S1.** <sup>1</sup>H and <sup>13</sup>C{<sup>1</sup>H} NMR spectra of **1** in CDCl<sub>3</sub>.

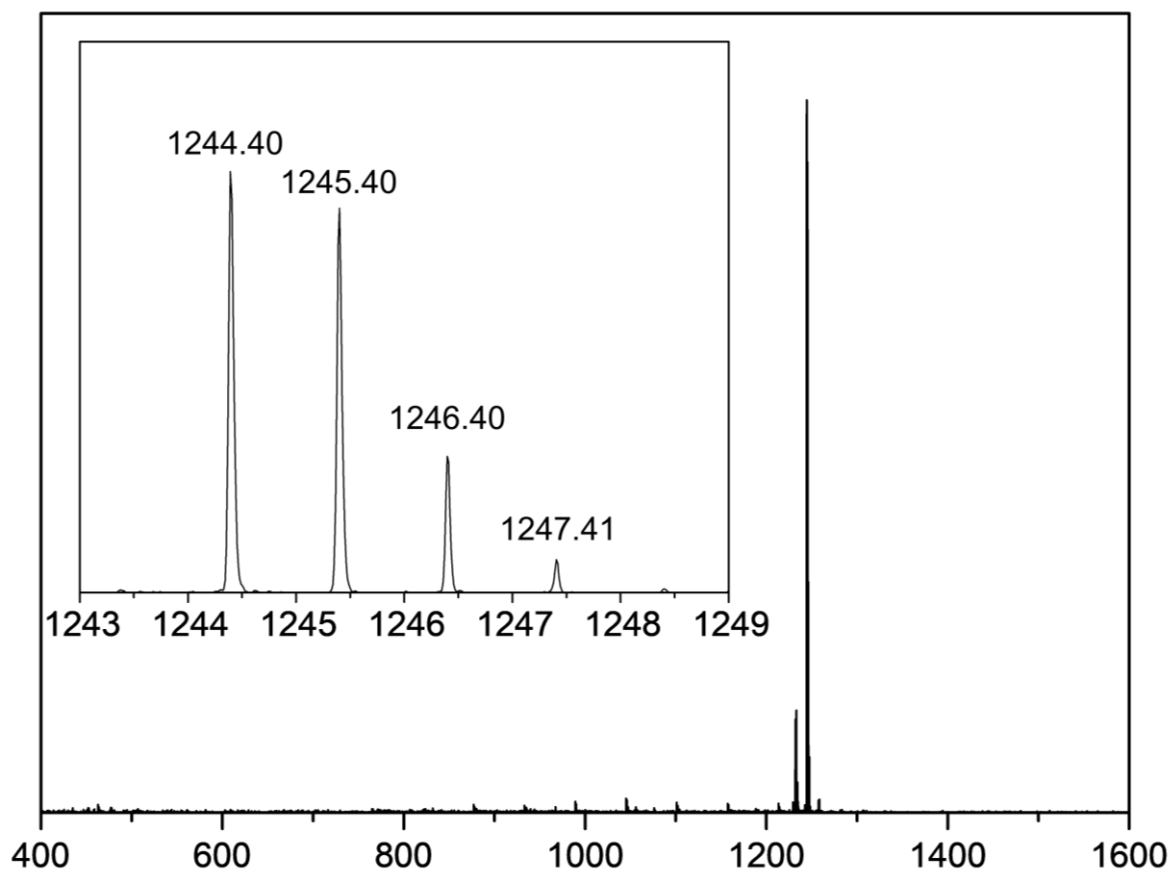


**Figure S2.** MALDI-TOF-MS spectrum of **1**.

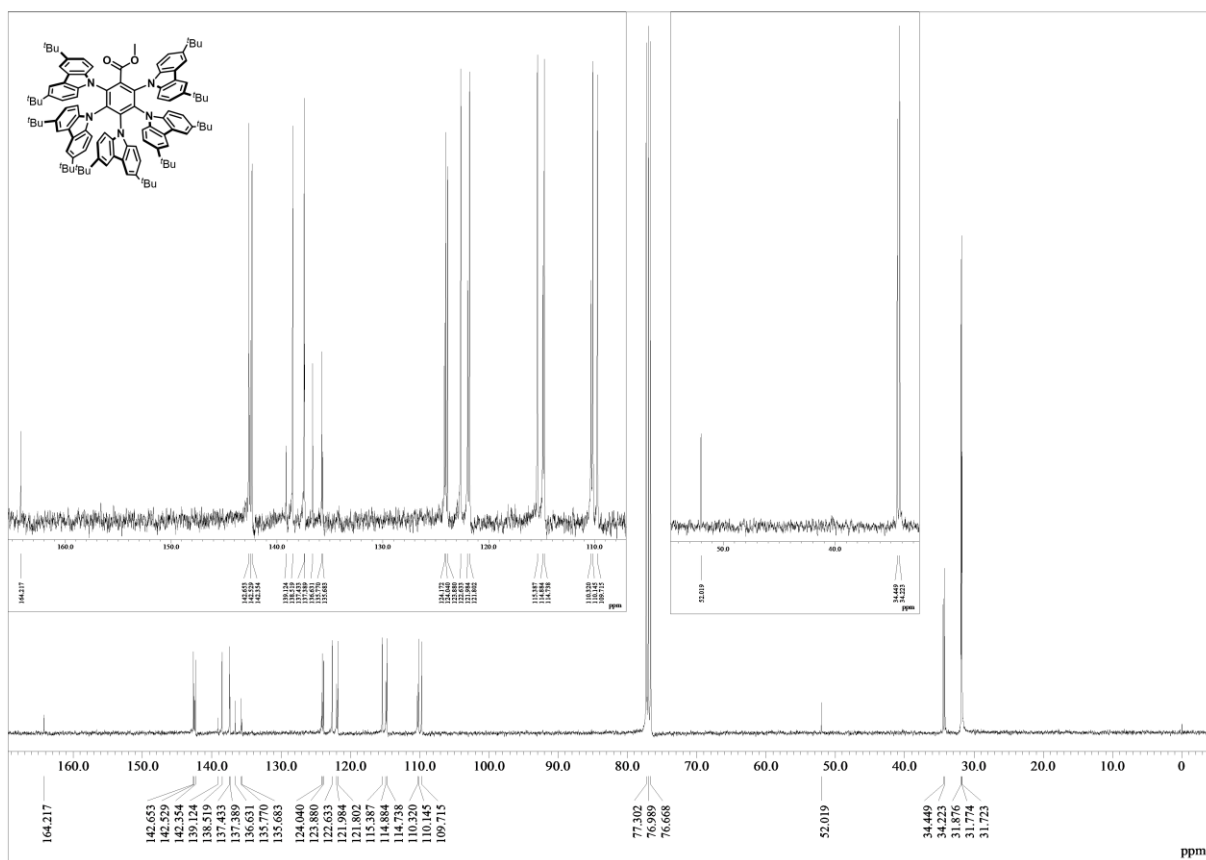
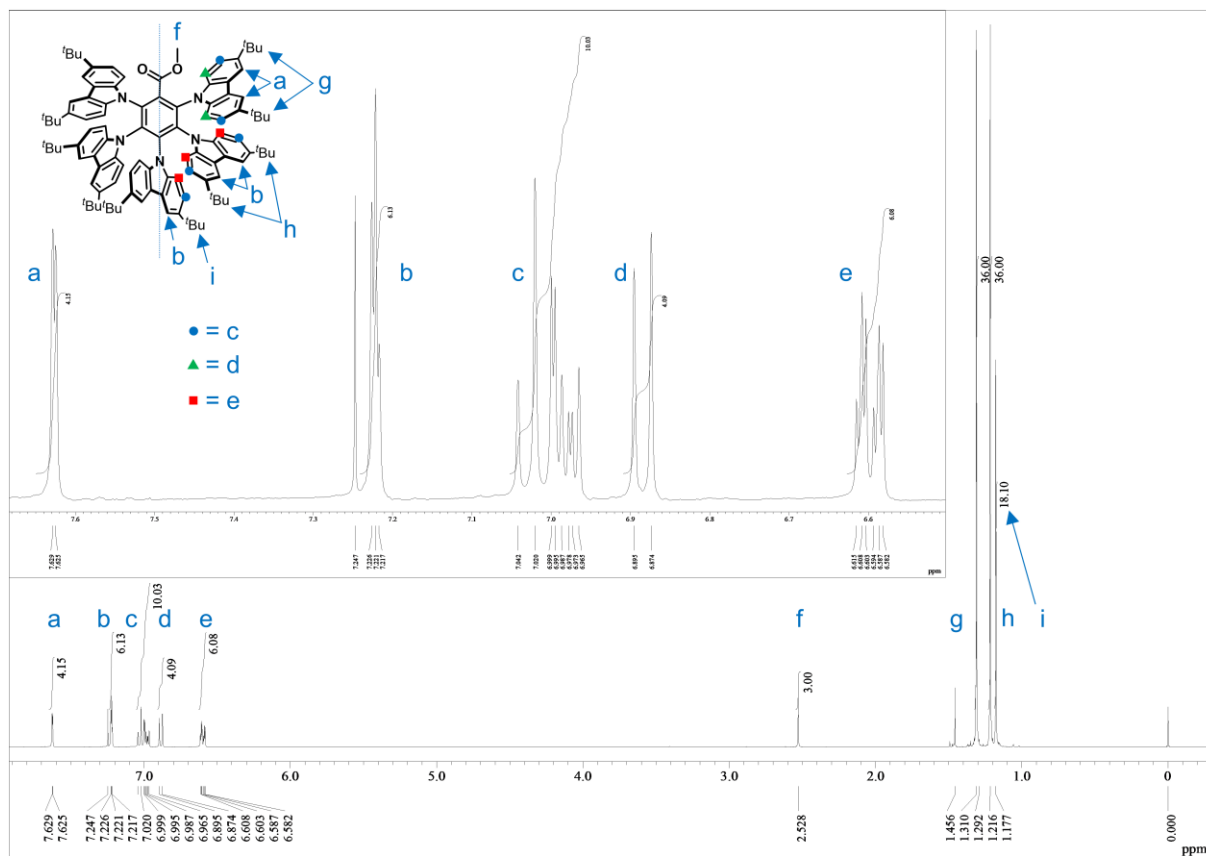


**Figure S3.** <sup>1</sup>H and <sup>13</sup>C{<sup>1</sup>H} NMR spectra of **2** in CDCl<sub>3</sub>.

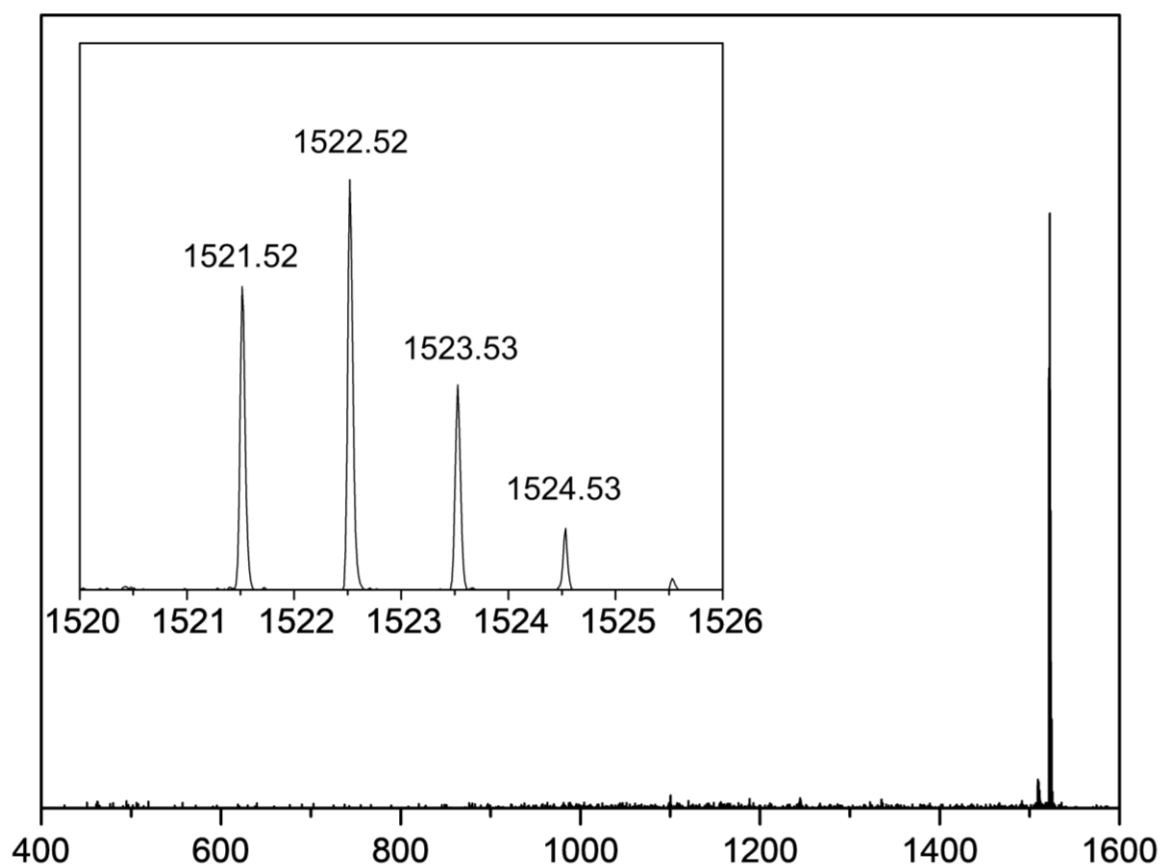


**Figure S4.** MALDI-TOF-MS spectrum of **2**.

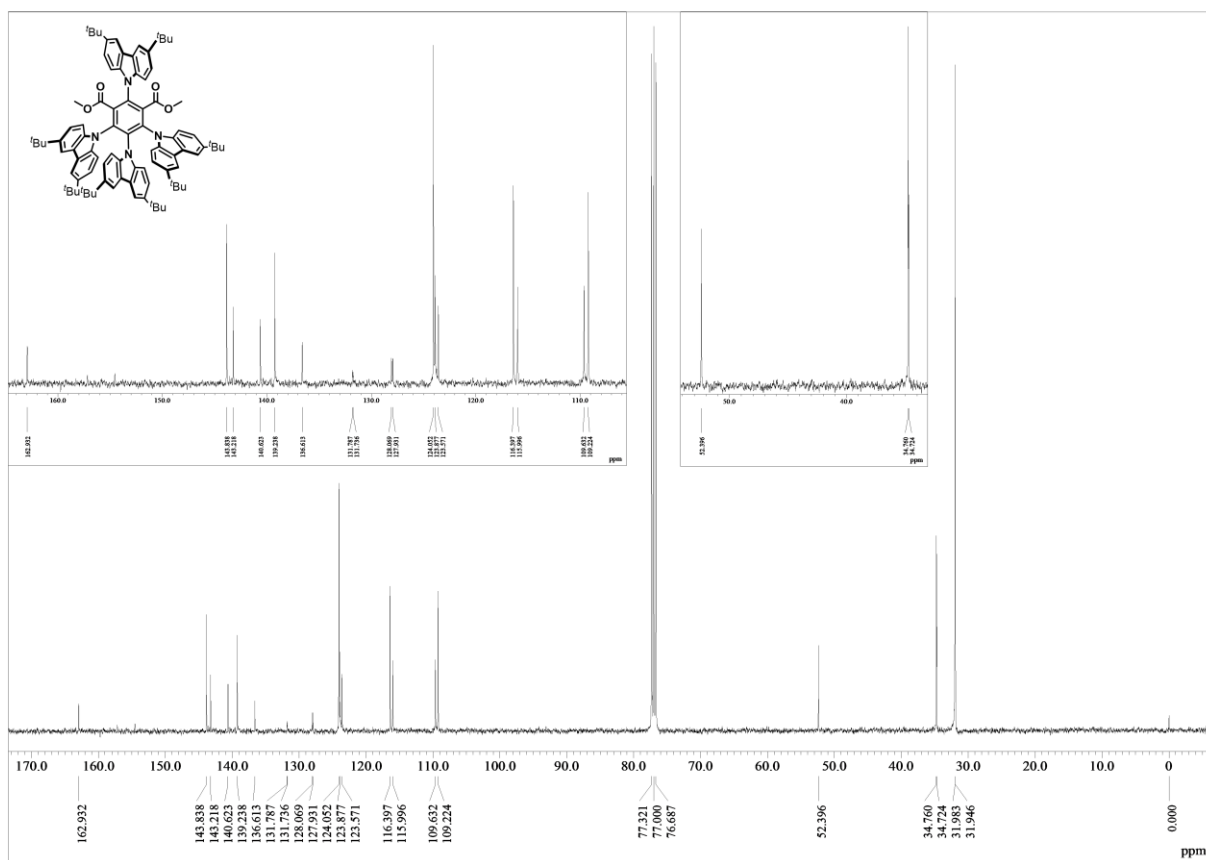
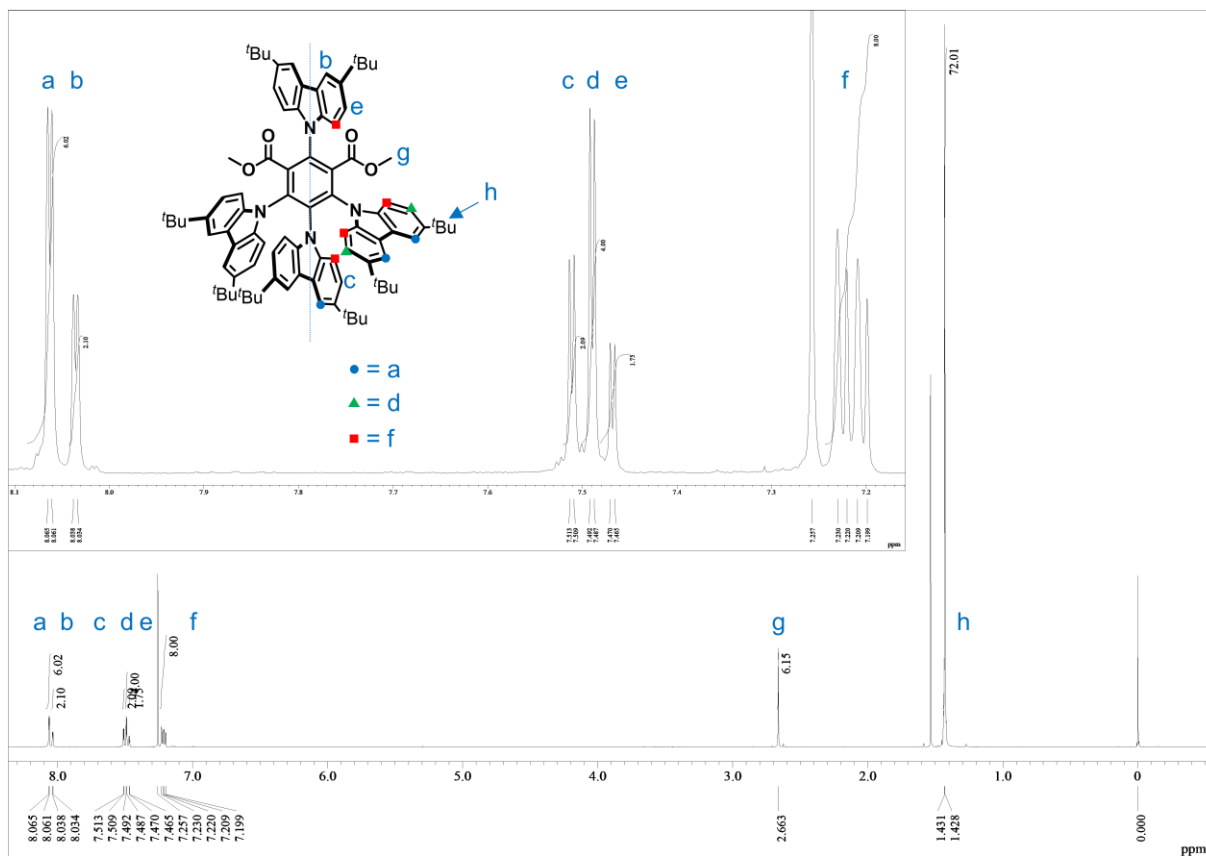


**Figure S5.** <sup>1</sup>H and <sup>13</sup>C{<sup>1</sup>H} NMR spectra of 3 in CDCl<sub>3</sub>.

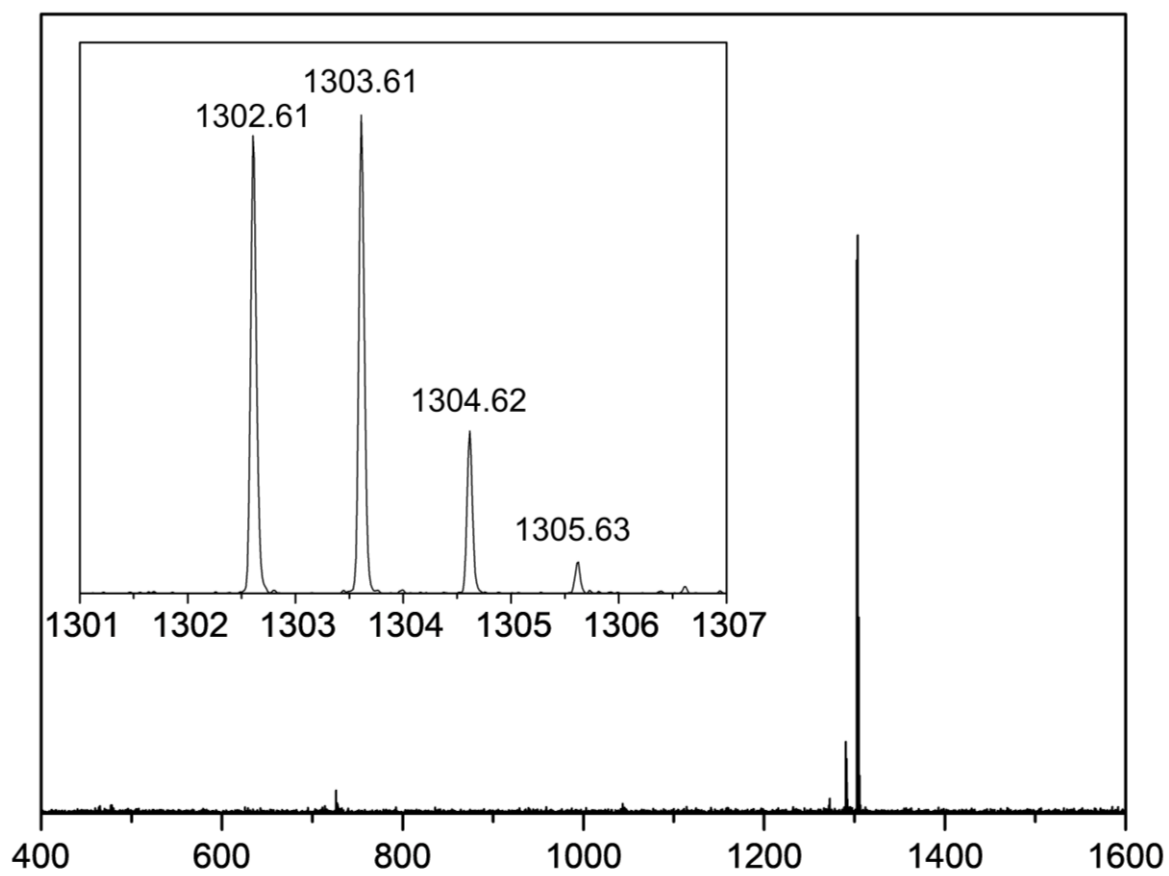


**Figure S6.** MALDI-TOF-MS spectrum of **3**.

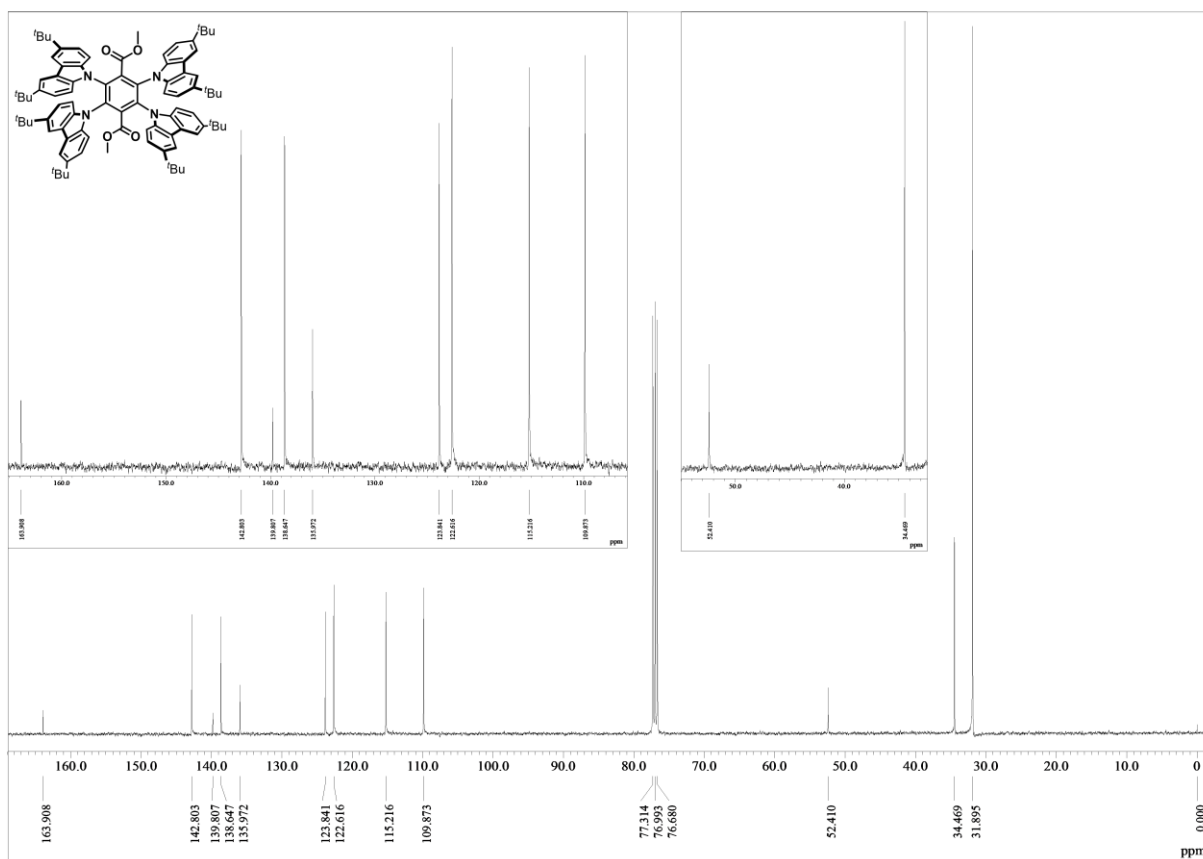
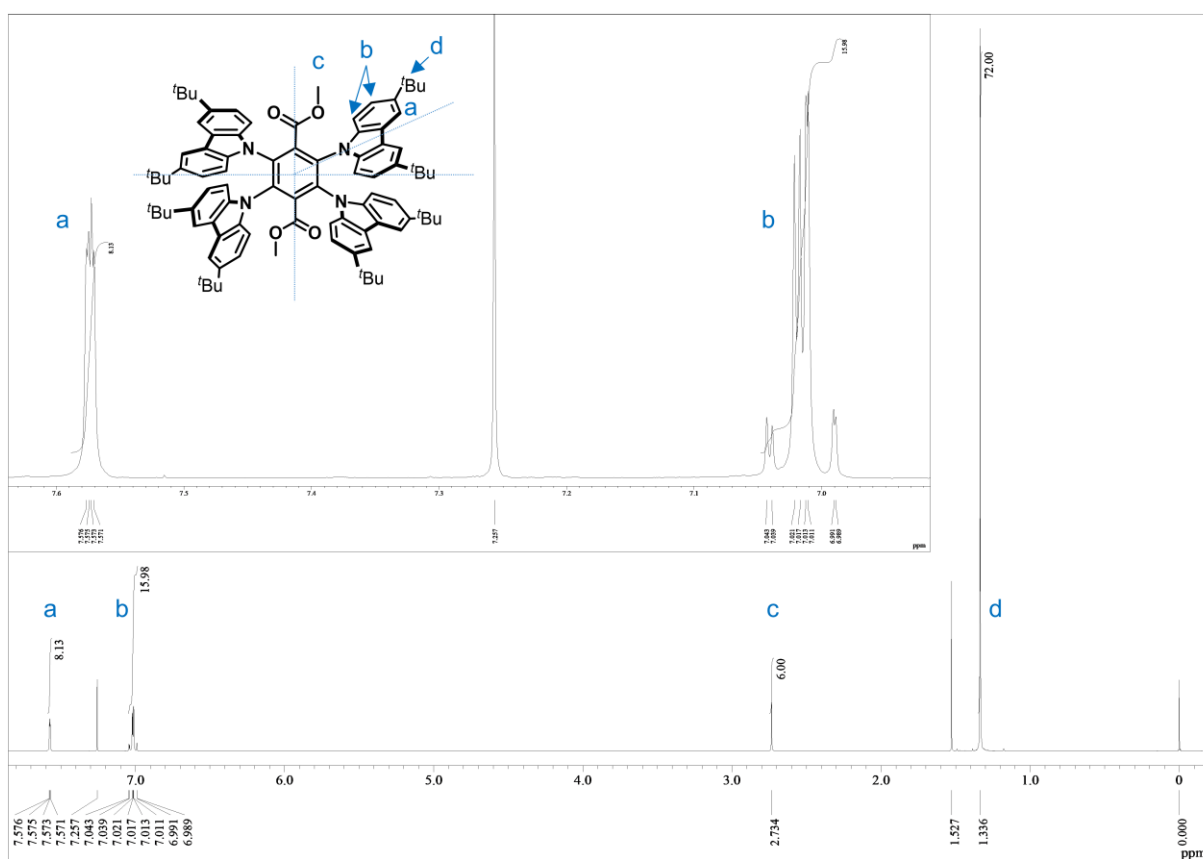


**Figure S7.** <sup>1</sup>H and <sup>13</sup>C{<sup>1</sup>H} NMR spectra of **4** in CDCl<sub>3</sub>.

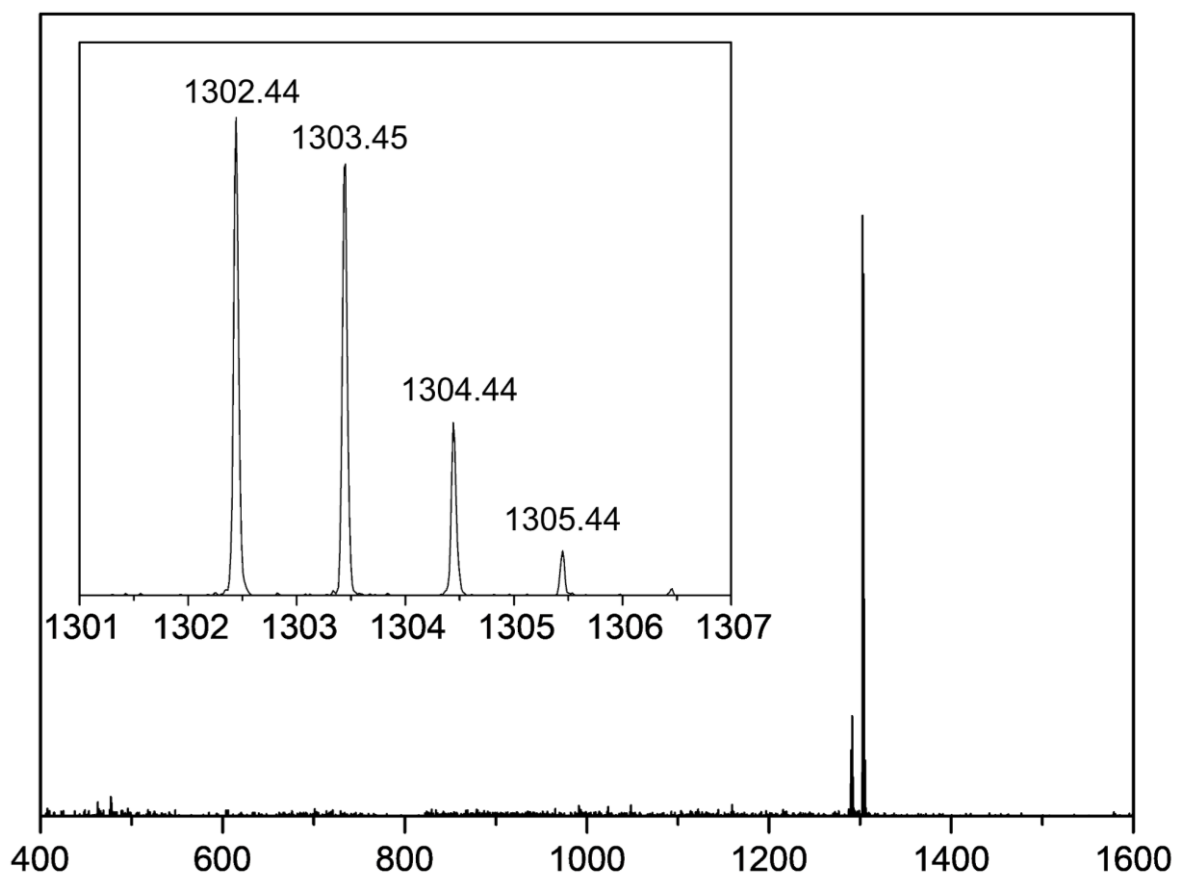


**Figure S8.** MALDI-TOF-MS spectrum of **4**.

		4BCzMB (1)	5BCzMB (2)	4BCzDMI (3)	4BCzDMT (4)
Emitter					
$S_1$ (eV)		2.648	2.580	2.503	2.343
$T_1$ (eV)		2.624	2.555	2.485	2.330
$\Delta E_{eg}$ (eV)		4.20	4.01	3.94	3.88
$\Delta E_{ST}$ (meV)		24	25	18	13
$f$		0.060	0.071	0.077	0.051
$\lambda_S$ (eV)		0.71	0.73	0.76	0.82
$\lambda_{PL}$ (nm)		468	481	499	529
$S_1$ geometry	LUNTO				
	HONTO				

**Figure S9.** Computational results of **1–4** calculated at the PBE0/6-31G(d) level.

		$S_0$	$S_1$			
Compound	State	$\theta_1$ [°]	$\theta_2$ [°]	$\theta_3$ [°]	$\theta_4$ [°]	$\theta_5$ [°]
<b>2</b>	$S_0$	62	63	60	62	60
	$S_1$	58	66	74	82	81
<b>5BCzBN</b>	$S_0$	66	62	60	61	66
	$S_1$	63	66	73	78	80

**Figure S10.** Representation of the structural differences between **2** and **5BCzBN**. Dihedral angle ( $\theta$ ) between the benzene core and ester (or nitrile) group at the  $S_0$  and  $S_1$  geometries were simulated using TD-DFT at the PBE0/6-31G(d) level.

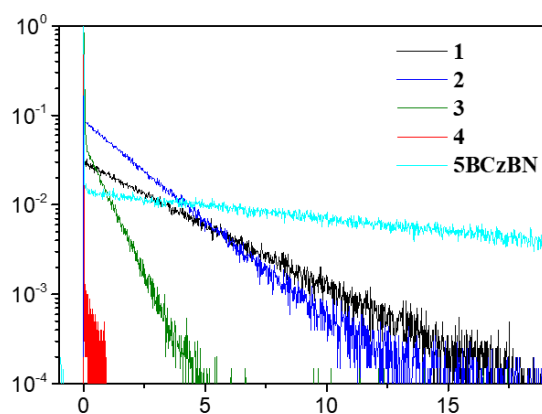


**Figure S11.** Transient PL decay profiles of **1–4** and **5BCzBN** in deoxygenated toluene solution at 300 K.

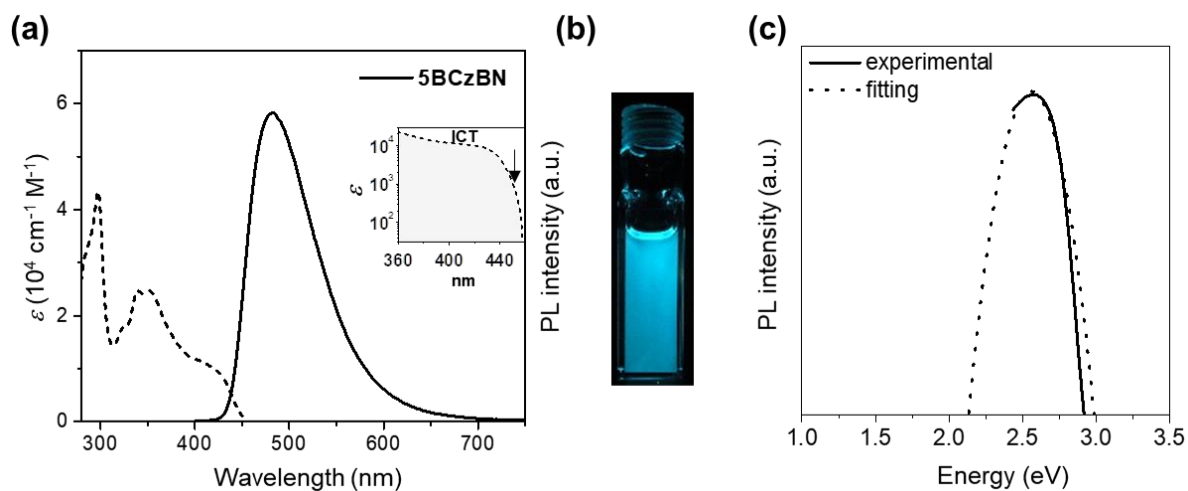


**Figure S12.** (a) UV–vis absorption and PL spectra of **5BCzBN** in toluene ( $10^{-5}$  M). The inset shows a magnified view of the ICT absorption band. (b) Photograph of the PL emission from the solution under UV irradiation. (c) PL spectrum (solid lines) fitted using Eq. (1) for the evaluation of  $\lambda_s$ .

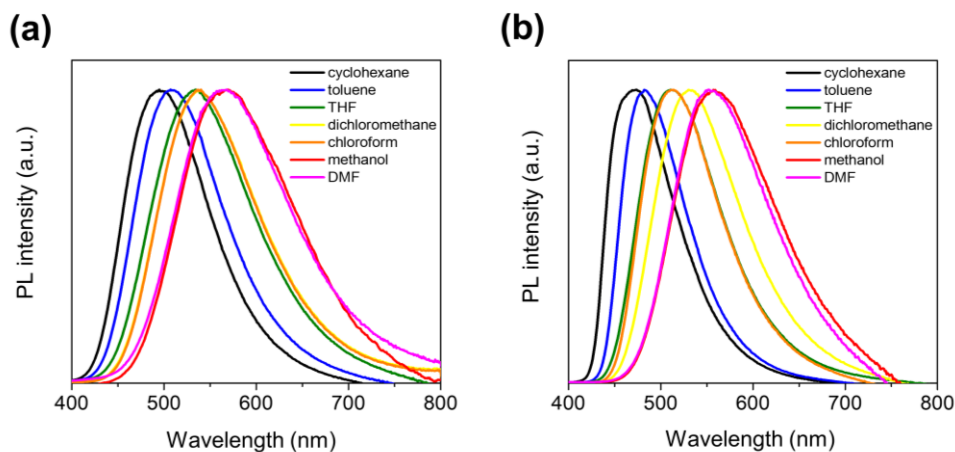


**Figure S13.** Solvatochromic PL properties of (a) **2** and (b) **5BCzBN** in various solvents with different polarities.

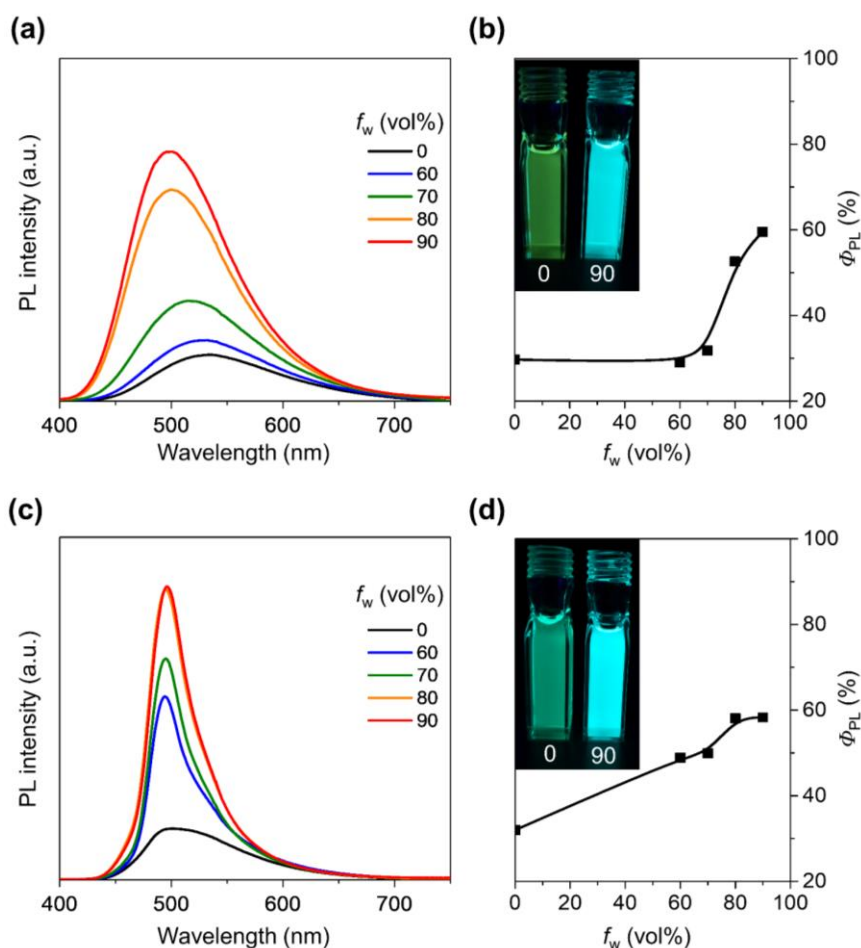


**Figure S14.** PL spectra of (a) **2** and (c) **5BCzBN** in THF/water mixtures with different water fractions ( $f_w$ ). Plots of absolute  $\Phi_{PL}$  vs.  $f_w$  for (b) **2** and (d) **5BCzBN** in the aqueous mixtures. Inset in (b) and (d): fluorescence images of **2** and **5BCzBN** in pure THF ( $f_w = 0\%$ ) and in a THF/water mixture ( $f_w = 90\%$ ) under UV light irradiation, respectively.

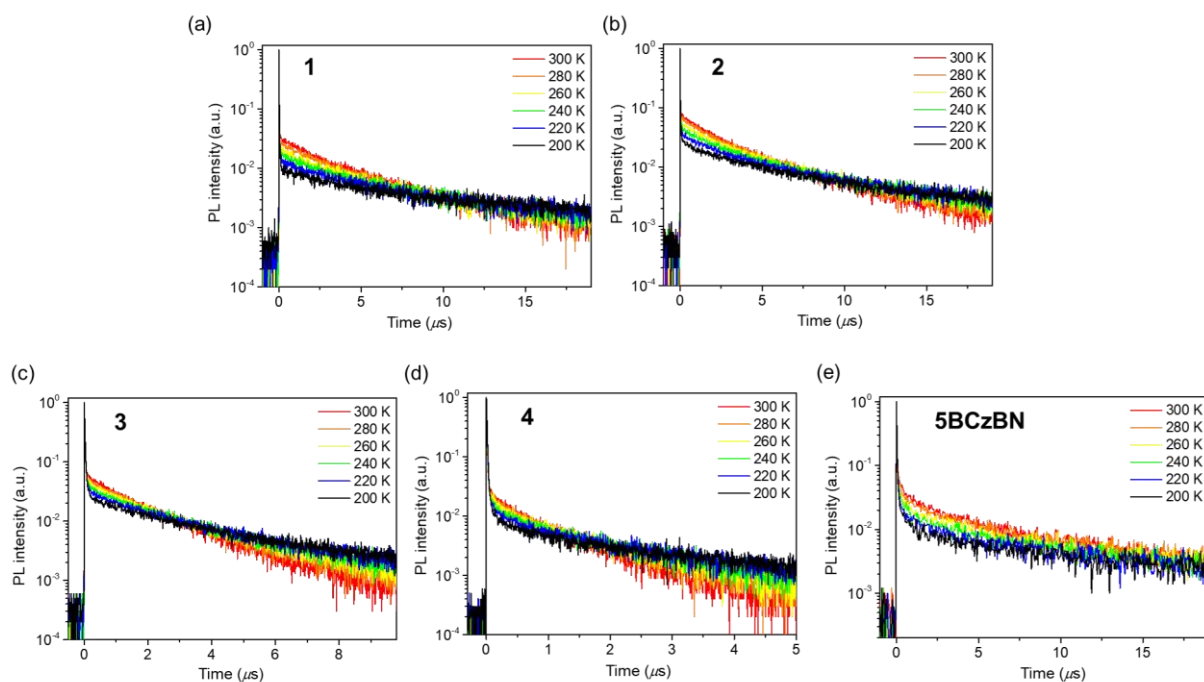


**Figure S15.** Transient PL decay curves of **1–4** and **5BCzBN** in the neat films measured at varying temperatures.

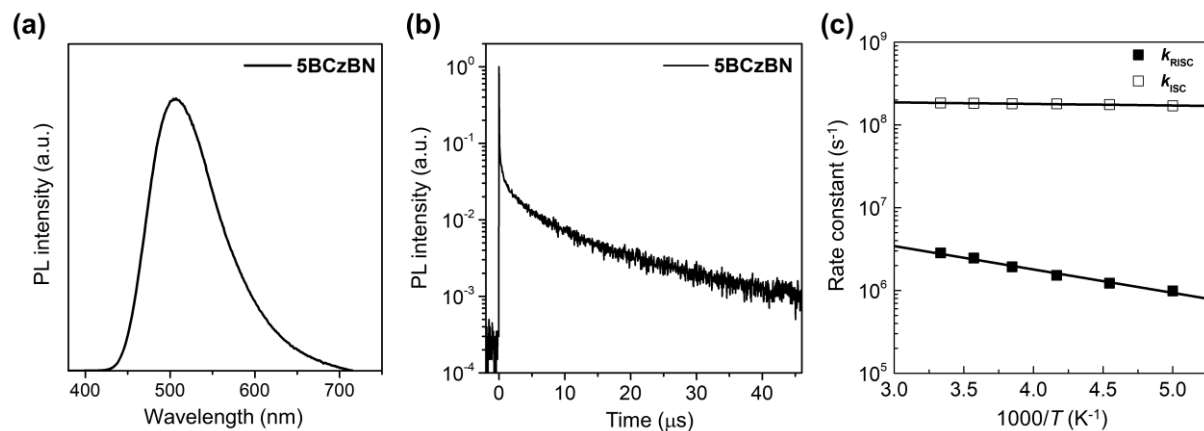


**Figure S16.** (a) Steady-state PL spectrum, (b) transient PL decay profile of **5BCzBN** in the neat film measured at 300 K under  $N_2$ . (c) Arrhenius plots of  $k_{ISC}$  and  $k_{RISC}$ , measured for the neat film of **5BCzBN**, where the solid lines denote the least-squares fittings.

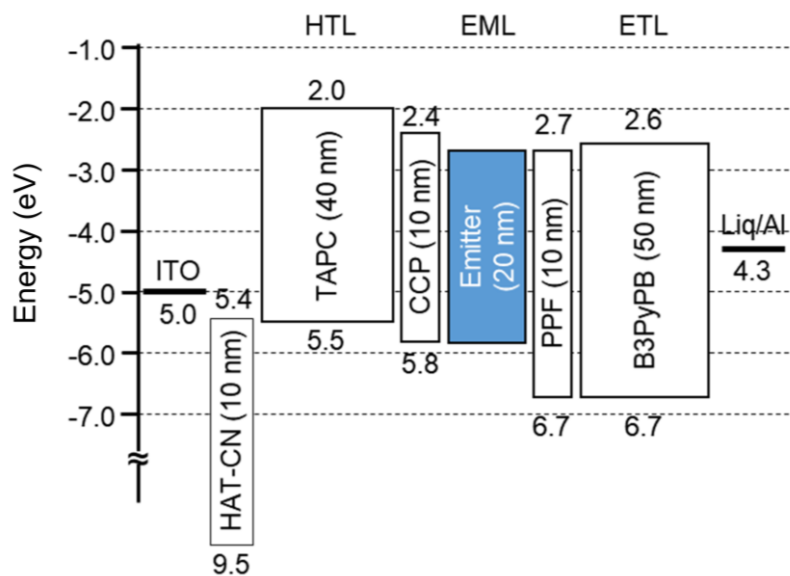


**Figure S17.** Energy-level diagram for the non-doped TADF-OLEDs (devices A–E).

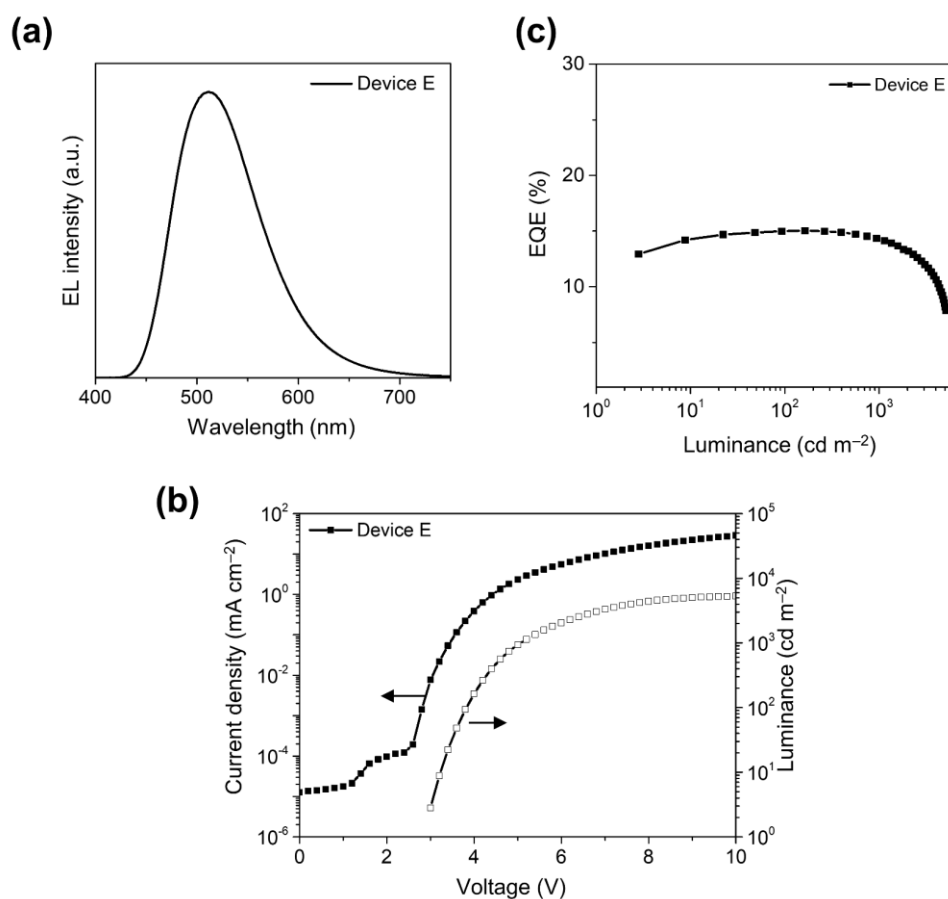


**Figure S18.** (a) EL spectrum, (b) current density–voltage–luminance ( $J$ – $V$ – $L$ ) characteristics, and (c) EQE vs.  $L$  plot of an OLED based on **5BCzBN** as an emitter (device E).

## References

- [S1] H. Sasabe, E. Gonmori, T. Chiba, Y.-J. Li, D. Tanaka, S.-J. Su, T. Takeda, Y.-J. Pu, K. Nakayama and J. Kido, *Chem. Mater.*, 2008, **20**, 5951.
- [S2] M. Numata, T. Yasuda and C. Adachi, *Chem. Commun.*, 2015, **51**, 9443.
- [S3] D. Zhang, M. Cai, Y. Zhang, D. Zhanga and L. Duan, *Mater. Horiz.*, 2016, **3**, 145.
- [S4] Gaussian 16, Revision A.03, M. J. Frisch, G. W. Trucks, H. B. Schlegel, G. E. Scuseria, M. A. Robb, J. R. Cheeseman, G. Scalmani, V. Barone, G. A. Petersson, H. Nakatsuji, X. Li, M. Caricato, A. V. Marenich, J. Bloino, B. G. Janesko, R. Gomperts, B. Mennucci, H. P. Hratchian, J. V. Ortiz, A. F. Izmaylov, J. L. Sonnenberg, D. Williams-Young, F. Ding, F. Lipparini, F. Egidi, J. Goings, B. Peng, A. Petrone, T. Henderson, D. Ranasinghe, V. G. Zakrzewski, J. Gao, N. Rega, G. Zheng, W. Liang, M. Hada, M. Ehara, K. Toyota, R. Fukuda, J. Hasegawa, M. Ishida, T. Nakajima, Y. Honda, O. Kitao, H. Nakai, T. Vreven, K. Throssell, J. A. Montgomery, Jr., J. E. Peralta, F. Ogliaro, M. J. Bearpark, J. J. Heyd, E. N. Brothers, K. N. Kudin, V. N. Staroverov, T. A. Keith, R. Kobayashi, J. Normand, K. Raghavachari, A. P. Rendell, J. C. Burant, S. S. Iyengar, J. Tomasi, M. Cossi, J. M. Millam, M. Klene, C. Adamo, R. Cammi, J. W. Ochterski, R. L. Martin, K. Morokuma, O. Farkas, J. B. Foresman, D. J. Fox, Gaussian, Inc., Wallingford CT, 2016.